

Nociception originating from the crural fascia in rats

Toru Taguchi^{a,*}, Masaya Yasui^b, Asako Kubo^{a,c}, Masahiro Abe^d, Hiroshi Kiyama^b, Akihiro Yamanaka^a, Kazue Mizumura^c

^a Department of Neuroscience II, Research Institute of Environmental Medicine, Nagoya University, Nagoya, Japan

^b Department of Functional Anatomy and Neuroscience, Nagoya University Graduate School of Medicine, Nagoya, Japan

^c Department of Physical Therapy, College of Life and Health Sciences, Chubu University, Kasugai, Japan

^d Medical Information Department, Vitacain Pharmaceutical Co. Ltd., Moriguchi, Japan

Sponsorships or competing interests that may be relevant to content are disclosed at the end of this article.

ARTICLE INFO

Article history:

Received 21 January 2013

Received in revised form 21 February 2013

Accepted 12 March 2013

Keywords:

Crural fascia

Nociceptors

Activity-dependent change in conduction velocity (ADCCV)

Twin pulse difference (TPD)

c-Fos

Peripherin

ABSTRACT

Little is documented in the literature as to the function of muscle fascia in nociception and pain. The aim of this study was to examine the distribution of presumptive nociceptive nerve fibers, to characterize fascial thin-fiber sensory receptors, and to examine the spinal projection of nociceptive input from the rat crural fascia (CF). Nerve fibers labeled with specific antibodies to calcitonin gene-related peptide (CGRP) and peripherin were found to be densely distributed in the distal third of the CF. Thin-fiber receptors (A δ - and C-fibers) responding to pinching stimuli to the CF with sharpened watchmaker's forceps, identified in vivo with the teased fiber technique from the common peroneal nerve, exist in the CF. Forty-three percent of the mechano-responsive fascial C-fibers were polymodal receptors (nociceptors) responding to mechanical, chemical (bradykinin), and heat stimuli, whereas almost all A δ -fibers were responsive only to mechanical stimuli. Repetitive pinching stimulus to the CF induced c-Fos protein expression in the middle to medial part of superficial layers ie, laminae I–II of the spinal dorsal horn at segments L2 to L4, peaking at L3. These results clearly demonstrate the following: 1) peptidergic and non-peptidergic axons of unmyelinated C-fibers with nerve terminals are distributed in the CF; 2) peripheral afferents responding to noxious stimuli exist in the fascia, and 3) nociceptive information from the CF is mainly processed in the spinal dorsal horn at the segments L2 to L4. These results together indicate that the "muscle fascia," a tissue often overlooked in pain research, can be an important source of nociception under normal conditions.

© 2013 International Association for the Study of Pain. Published by Elsevier B.V. All rights reserved.

1. Introduction

Muscle fascia is less documented in the literature except for the biomechanical properties, although it has long been considered not only an important source of nociception and pain but also a critical target for treatment of musculoskeletal pain [11]. Musculoskeletal pain is of greater clinical importance than cutaneous pain because of its higher prevalence, persistent nature, impact on activities in daily living, and other effects [16,19]. It is only recently, however, that musculoskeletal pain has come to be more appreciated. Indeed, the International Association for the Study of Pain (IASP) selected "musculoskeletal pain" as a theme for a Global Year Campaign (Oct. 2009–Oct. 2010). The "second skeleton," fascia,

however, continues to be largely ignored even in the field of musculoskeletal pain research, and even after this campaign.

We have systematically investigated the spinal dorsal horn neurons receiving input from the thoracolumbar fascia (TLF) in rats [10,27], and found that the proportion of second-order neurons with fascial input from the TLF significantly increased in animals with chronic myositis in the low back. The TLF is presumably innervated by nociceptive nerve fibers both in rats and in humans [34]. In human subjects with delayed-onset muscle soreness (DOMS) after lengthening contraction of the leg, the fascia, presumably the crural fascia (CF) covering the tibialis anterior muscle, reportedly became more sensitive to noxious stimulus than the exercised muscle itself [9], although in an animal model of DOMS muscular nociceptors were also sensitized to mechanical stimulation [30]. It has been reported that a localized sensitive spot is formed at a restricted depth in fascia in experimental models of DOMS after lengthening contraction in rabbits and in humans [12,13]. In addition, nerve growth factor, a neurotrophic and survival factor for sensory neurons during development, and now

* Corresponding author. Address: Department of Neuroscience II, Research Institute of Environmental Medicine, Nagoya University, Furo-cho, Chikusa-ku, Nagoya 464-8601, Japan. Tel.: +81 52 789 3862; fax: +81 52 789 3889.

E-mail address: tagu@riem.nagoya-u.ac.jp (T. Taguchi).

known to be involved in inflammatory hyperalgesia in adulthood, induced a lasting increase in the sensitivity of the muscle fascia at the lumbar level to mechanical and chemical stimuli [5]. These recent articles suggest not only that the muscle fascia could be a source of nociception in a physiological condition, but also that it could play crucial roles in hyperalgesic conditions (eg, myofascial pain syndrome). However the role of fascia as a nociceptive organ has not been fully established. Only 1 article has addressed peripheral fascial nociceptors with receptive fields in the low back, and their conductive and receptive properties have not been clarified in detail [1].

Recently, *ex vivo* single-fiber recordings revealed that not only receptive properties but also axonal conductive properties of thin-fiber receptors, as shown by activity-dependent change of conduction velocity (ADCCV) and twin pulse difference (TPD), are useful in understanding peripheral mechanisms of nociception and pain [8,23,35]. ADCCV in particular exhibits a functional link to receptive properties of nociceptors [4,29].

Here we examined the following: 1) the distribution of presumptive nociceptive nerve fibers in the CF; 2) axonal and receptive characteristics of peripheral thin-fiber afferents with receptive fields in the CF; and 3) the spinal projection of nociceptive input originating from the CF.

A preliminary account appeared elsewhere [32].

2. Methods

2.1. Animals

A total of 42 male Sprague-Dawley rats (SLC Inc., Shizuoka, Japan), 8 to 14 weeks of age and 280 to 450 g, were used in this study. The animals were kept 1 to 3 per cage in a clean room with air-conditioning (temperature, 23°C) under a 12-hour light/dark cycle (light between 08.00/09.00 and 20.00/21.00 h). The animals had free access to food and filtered clean water until the final experiment. The present study was conducted in its entirety according to the Regulations for Animal Experiments in Nagoya University, the Fundamental Guidelines for Proper Conduct of Animal Experiments and Related Activities in Academic Research Institutions in Japan, and the Ethical Guidelines of the International Association for the Study of Pain [39].

2.2. Immunohistochemical labeling of nerve fibers in crural fascia

Under deep anesthesia with sodium pentobarbital (80 mg/kg, *i.p.*), the animals were perfused with 0.1 M phosphate buffered saline (PBS) and fixed with 4% paraformaldehyde in PBS. The CF was quickly excised and removed from anterior lower legs. Whole-mount fascia preparations ($n = 4-5$) were made to examine the distribution of nerve fibers and the terminals in the CF. Transverse sections of the CF ($n = 6$) were also made to measure the length and number of labeled nerve fibers for quantitative analysis. The whole mount preparations were incubated overnight at room temperature (RT) with primary antibodies against protein gene product 9.5 (PGP 9.5, $n = 4$, 1:1,000, RA95101, UCL, Isle of Wight, UK), CGRP ($n = 5$, 1:1,000, polyclonal rabbit antibody to CGRP, C8198, Sigma, St. Louis, MO), or peripherin ($n = 5$, 1:1,000, polyclonal rabbit antibody to peripherin, AB1530, Millipore, MA). After washing, the preparations were incubated with a secondary antibody (1:200, BA-1000, Vector Laboratories, CA) for 3 hours at RT. In the transverse sections, the primary antibodies were incubated for 2 days at 4°C. For quantitative analysis, transverse sections 20 μm in thickness were cut in the proximal, middle, and distal third of the CF. Six sections from the 6 different preparations (ie, 1 section from each preparation), were analyzed in each part of

the CF. Immunoreactive nerve fibers and their terminals were traced and counted with a light microscope-equipped and computer-aided imaging system at a magnifying power of $\times 200$, or in some cases $\times 400$ (NeuroLucida, MicroBrightfield, Williston, VT). The most final end or the finest tip of a nerve fiber at the peripheral terminal in the CF, which was obviously different from a cut end with a relatively broader diameter, was considered to be a nerve terminal.

2.3. Electrophysiology

2.3.1. General surgical procedures

The animals were deeply anesthetized with sodium pentobarbital (50 mg/kg *i.p.* initially), followed by an *i.v.* infusion of the same anesthetic as above at a constant rate (approximately one-third of the initial dose per hour) using an infusion pump (ESP-64, Eicom Corp., Kyoto, Japan) to maintain a deep and constant level of anesthesia during the experiment. A catheter was inserted into the right external jugular vein for administration of the anesthetic and a muscle relaxant. The anesthesia was kept deep enough to abolish flexor reflexes and marked blood pressure changes (exceeding 10 mmHg) to noxious pinching of the tail. The electrocardiogram was monitored, and the depth of the anesthesia was adjusted so that the heart rate did not exceed 430 beats per minute. The muscle relaxant (pancuronium bromide, Mioblock, Schering-Plough, Osaka, Japan) was used to immobilize the animals (0.6–0.8 mg/h/rat *i.v.*). Another catheter was inserted into the right common carotid artery to measure blood pressure (mean arterial blood pressure >80 mmHg). The animals were put on a thermal blanket with feedback regulation (ATB-1100, Nihon Kohden Corp., Tokyo, Japan), left-side up, to monitor and maintain rectal temperature at a physiological level (37–38°C). Artificial ventilation was performed via a tracheal cannula with a gas mixture of 47.5% O₂, 2.5% CO₂, and 50% N₂ (arterial pO₂ of >100 mmHg, pCO₂ of 32–40 mmHg, pH close to 7.4) [10,27]. The skin was cut laterally along the femur and the fibula between the iscial tuberosity and the lateral malleolus. The skin flap from this was used to make a pool with paraffin oil to cover the recording site and the exposed CF (Fig. 1).

2.3.2. Recordings of thin-fiber receptors

A teased fiber technique was used to obtain the activities of a single fascial thin-fiber receptor from the common peroneal nerve *in vivo* (Fig. 1). First a mechanically sensitive receptive field (RF) was roughly searched by manual pinching of the CF with blunt forceps. Then the exact distribution (size and location) of the RF was defined with sharpened watchmaker's forceps, and mapped on a standardized chart. The CF alone could be stimulated separately from the muscle underneath because it has sufficient thickness and is connected to the muscle with a loose connective tissue. The size of the RF was measured by calculating the number of pixels in the RF that was drawn on the chart with ImageJ software from the National Institutes of Health (<http://rsbweb.nih.gov/ij/index.html> available online). Action potentials were analyzed on a computer with the DAPSYS data acquisition system (<http://www.dapsys.net>; Brian Turnquist, turnquist@bethel.edu) [38].

When a single fiber was identified, the RF was stimulated with twin rectangular electric pulses via a bipolar stimulating electrode placed beside the center of the RF (pulse duration: 500 μs , inter-stimulus interval: 50 ms, frequency: 0.5 Hz, repetitions: 6, and stimulus intensity: 1–2 times the threshold (range: 1.8–40 V) (Fig. 2) to observe axonal conductive properties of fascial thin-fiber receptors using the indices of activity-dependent change in conduction velocity (ADCCV) and twin pulse differences (TPD). The usefulness and method for calculation of these indices have been reported in recent articles [6,23,29].

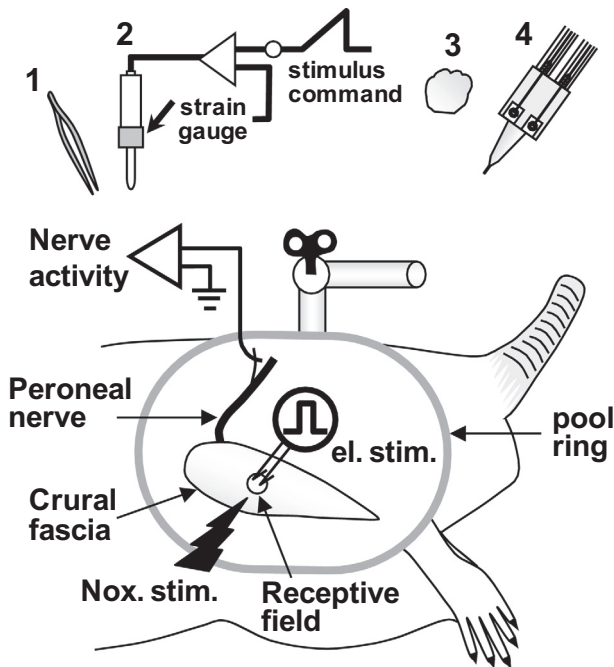


Fig. 1. Experimental set-up for single-fiber recording of fascial thin-fiber receptors. The recording was made from the common peroneal nerve innervating the CF of rats with the teased fiber technique *in vivo*. After the identification of a fiber, a series of noxious stimuli were applied to the identified receptive field in the CF: 1) noxious pinching; 2) force-controlled mechanical stimulus (ramp 0–392 mN/40 s); 3) chemical stimulus with a small cotton ball soaked with bradykinin 10 μ M; and 4) cold and heat stimuli (cooled from 32°C to 8°C in 40 seconds, and warmed from 32°C to 50°C in 30 seconds).

An original recording of ADCCV and TPD is shown in Fig. 2A. Each twin stimulus of a fiber induced double action potentials. Latencies of the action potentials induced by the first and second rectangular pulses gradually changed over the 6 repetitions (from twin stimulus 1 to 6) delivered every 2 seconds (Fig. 2B and C). The ADCCV of a fiber obtained by the first rectangular pulse of the twin stimuli is shown in Fig. 2D. The value of ADCCV was calculated from the CV according to the following formula:

$$\text{ADCCV (\%)} = \left[\frac{\{\text{CV measured by the first rectangular pulse of each twin stimulus (m/s)}\}}{\{\text{CV measured by the first rectangular pulse of twin stimulus 1 (m/s)}\}} \right] \times 100 - 100$$

Here, ADCCV with a negative value (%) means the slowing of CV compared with the CV obtained by twin stimulus 1. Similarly, ADCCV with a positive value (%) means the speeding of CV.

The value of TPD was calculated from the CV obtained by the first and second rectangular pulses of each twin stimulus (from 1 to 6 [example in Fig. 2E]) according to the following formula:

$$\text{TPD (\%)} = \left[\frac{\{\text{CV measured by the second rectangular pulse (m/s)}\}}{\{\text{CV measured by the first rectangular pulse (m/s)}\}} \right] \times 100 - 100$$

Here, TPD with a negative value (%) means the slowing of CV compared with the CV obtained by the first rectangular pulse of the twin stimuli. Similarly, TPD with a positive value (%) means the speeding of CV.

All data were stored on a magnetic tape for later off-line analysis and in a computer via an A/D converter (Power Lab/16s, ADInstruments) with sampling frequency of 20 kHz. Conduction velocity of thin-fiber receptors was calculated from the distance and conduction latency of an action potential induced by the first

rectangular pulse of twin stimulus 1. Fibers with CV of <2.0 m/s were classified as C-fibers, whereas those with CV of 2 to 20 m/s were classified as A δ -fibers [14]. Fibers with CV of >20 m/s were not included in the current experiment.

If a fiber responded to search mechanical stimulation, quantitative mechanical, chemical, and thermal (cold and heat) stimulations were applied to the identified RF in the following order: 1) a ramp mechanical stimulation with a servo-controlled mechanical stimulator, 2) bradykinin 10 μ M, 3) cold (cooled from approximately 32°C to 8°C), and 4) heat (heated from approximately 32°C to 50°C). Intervals between stimuli varied: when a stimulus induced no excitation, the interval before the next stimulus was set at about 5 minutes. When a stimulus induced an excitation, this 5-minute interval was begun from the end of the response.

2.3.3. Mechanical stimulation

For quantitative analysis of the mechanical sensitivity of a fiber, mechanical stimulus was applied by a mechanical stimulator with feedback regulation of the force (PS-2001, manufactured by S. Aizawa, Goto College of Medical Arts and Science, Tokyo, Japan). The stimulator has a plastic cylindrical probe with a flat circular tip (tip size: 2.28 mm²). A ramp mechanical stimulus, linearly increasing from 0 to 392 mN in 40 seconds, was applied to the most sensitive point of the identified RF. We used the same response criteria as in our previous study with muscular and cutaneous afferents to determine whether a tested fiber was responsive to a stimulus [29,30]. Specifically, a fiber was defined to be sensitive to a stimulus when it fulfilled the following criteria: 1) the net increase in the discharge rate during the stimulus period (40 seconds) was more than 0.1 imp/s above the background discharge rate during the control period (60 seconds) immediately before the mechanical stimulus; and 2) the instantaneous discharge rate of 2 consecutive discharges exceeded the mean + 2 SD of the background discharge rate. The mechanical threshold was defined as the intensity that induced a discharge that exceeded the mean frequency + 2 SD of background discharges during the control period (60 seconds), with 2 or more consecutive discharges exceeding this level. If a fiber showed no action potentials above the response criteria with mechanical stimulus up to 392 mN even though it exhibited firing in response to manual pinching with watchmaker's forceps, then the mechanical threshold was defined as 392 mN.

2.3.4. Chemical and thermal stimulations

Bradykinin (10 μ M, Peptide Institute, Inc., Osaka, Japan) was applied as an algescic chemical stimulus by putting a small cotton ball soaked with the solution directly on the CF. Next, thermal stimuli were applied to the fascial RF using a feedback-controlled Peltier thermode (UDH-300, Unique Medical Co., Ltd., Tokyo, Japan) with a small probe (diameter: 1 mm). From a baseline temperature of 32°C, the RF was gradually cooled to 8°C over 40 seconds or gradually heated to 50°C over 30 seconds at a constant rate of 0.6°C/s.

The same response criteria for chemical and thermal stimulations were used as in our previous article [29,30]. Namely, a fiber was defined to be sensitive to a stimulus when it fulfilled the following criteria: 1) the net increase in the discharge rate during the application period of 60 seconds, 40 seconds, and 30 seconds for bradykinin, cold, and heat, respectively, was more than 0.1 imp/s above the background discharge rate during the control period (60 seconds) immediately before application; and 2) the instantaneous discharge rate of 2 consecutive discharges exceeded the mean + 2 SD of the background discharge rate. The onset (latency) of the response was defined as the time when a fiber induced 2 or more consecutive discharges exceeding the mean frequency + 2 SD of the background discharge rate during the control period (60 seconds).

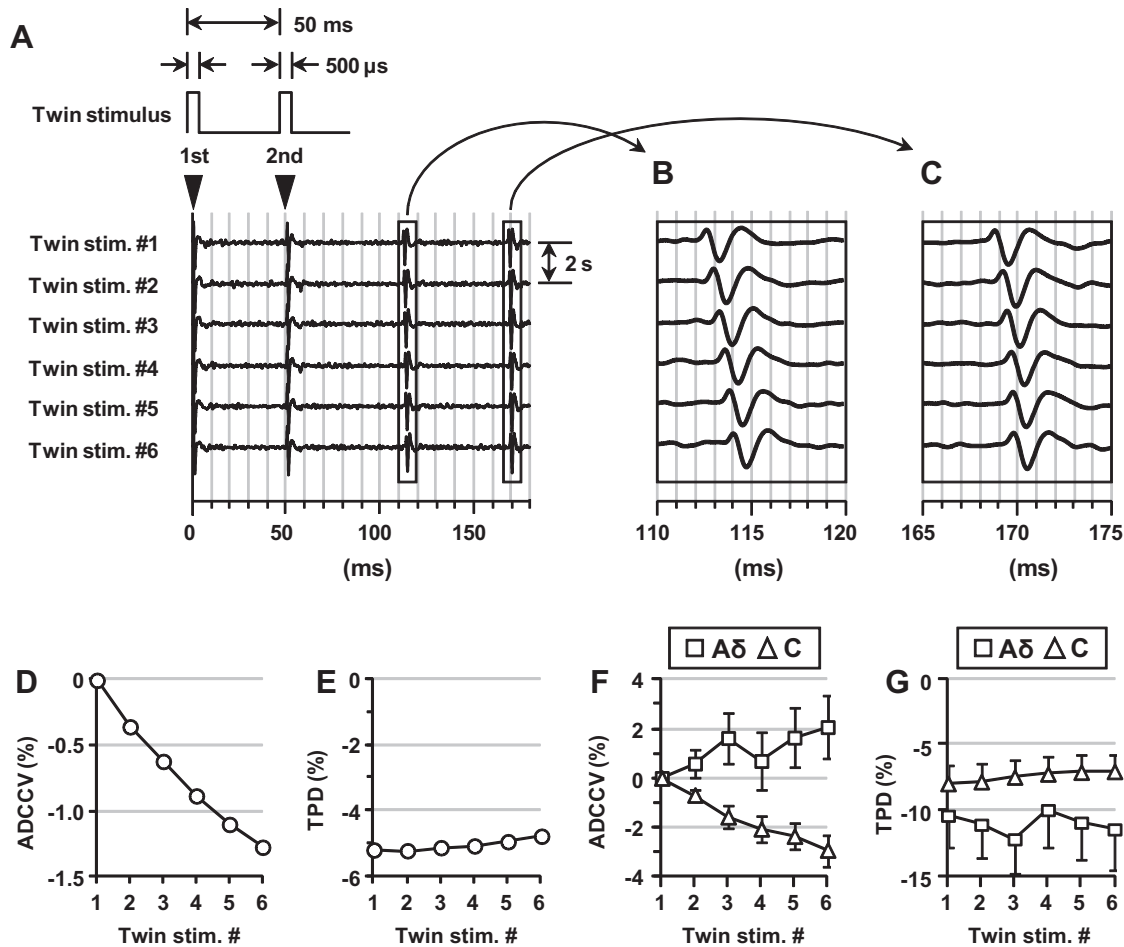


Fig. 2. Activity-dependent change of conduction velocity (ADCCV) and twin pulse difference (TPD). (A) A waterfall image of the original recording in the twin stimulus paradigm. Here the receptive field was stimulated with twin rectangular pulses via a bipolar stimulating electrode (pulse duration 500 μ s, inter-stimulus interval 50 ms, 6 repetitions (one every 2 s), and stimulus intensity 8 V) to observe ADCCV and TPD of a fiber. (B and C) The conduction latency tracking of the fiber evoked by the first (B) and second (C) rectangular pulses with an expanded time scale. Note a clear slowing of CV. The distance between the stimulating and recording electrodes was 56 mm. Conduction velocity calculated by the first rectangular pulse of the first twin stimulus was 0.50 m/s. (D) ADCCV of the fiber in A. (E) Changes in the TPD of the fiber in A. See Methods for details on the calculation of ADCCV and TPD. (F) Averaged patterns of ADCCV. Note a gradual slowing of CV in C-fibers ($n = 31$) over the 6 repetitions (twin stim. #1 to #6), whereas A δ -fibers ($n = 24$) showed a speeding rather than a slowing. Note that the pattern of ADCCV was significantly different between A δ - and C-fibers ($P < 0.001$, 2-way ANOVA). (G) Averaged patterns of TPD over the 6 repetitions (twin stim. #1 to #6). Note a significantly larger TPD in A δ -fibers ($n = 24$) compared with C-fibers ($n = 31$) ($P < 0.01$, 2-way ANOVA).

2.4. c-Fos study

Ten animals were assigned to the PINCH ($n = 5$) or SHAM ($n = 5$) group. Under deep anesthesia with urethane (initial dose of 1.5 g/kg, i.p.), the anterior surface of the skin in the right lower leg was further anesthetized with local anesthetic cream (EMLA cream containing 25 mg lidocaine + 25 mg prilocaine per 1 g; AstraZeneca Inc., London, UK) for 20 minutes to block nociceptive afferent input from the skin [20]. The CF was carefully exposed by excising the anesthetized skin after the cream was removed. Serrated forceps (type: 11627-12, Fine Science Tools Inc., CA) were used to apply a noxious mechanical stimulus (pinch) restricted to the CF, not reaching the muscle underneath the fascia. This was possible because the CF is thick and loosely connected to the muscle with connective tissues. The pinching stimulus, which was quite painful when applied to the experimenter's hand, was repeatedly applied to 18 defined points in the CF for 30 minutes (6 points from proximal to distal \times 3 lines medially and laterally, pinch for 5 seconds followed by a 5-second rest period). These procedures were performed with rectal temperature controlled at 37–39°C with a heating blanket. The CF was covered with paraffin oil to prevent drying of the tissue until perfusion and fixation. Animals that did not

receive pinching stimuli but underwent the other procedures (ie, urethane anesthesia, EMLA cream, and cutting the skin to expose the CF) were used as a SHAM control.

Two hours after the end of the stimulus protocol with or without pinching of the CF, the animals were deeply anesthetized with sodium pentobarbital (80 mg/kg, i.p.) and then perfused transcardially with physiological saline containing heparin sodium (1 unit/mL, Ajinomoto, Pharmaceuticals Co. Ltd., Tokyo, Japan) followed by 2% paraformaldehyde with 0.2% picric acid in 0.1 M PBS. The lumbar spinal cord was quickly removed, post-fixed overnight in the same fixative, and cryoprotected in 20% sucrose dissolved in PBS for a few days. Transverse frozen sections (40 μ m) of the spinal cord from L1 to L5 were cut with a microtome, and every fourth section was used for analysis.

Immunohistochemical staining of c-Fos was performed according to our previous protocol [28]. Briefly, after blocking endogenous peroxidase activity with 0.3% hydrogen peroxide, sections were processed for immunohistochemistry with the free-floating ABC technique using polyclonal rabbit antibody to c-Fos (1:5000, sc-52, Santa Cruz Biotechnology, Santa Cruz, CA), biotinylated goat anti-rabbit immunoglobulin (1:500, BA-1000, Vector Laboratories, Burlingame, CA) and avidin-biotin complex (PK-6100, Vector Laboratories). Finally, sections were

reacted in a 0.05 M Tris-buffer (pH 7.6) containing 0.02% 3,3'-diaminobenzidine tetrahydrochloride (DAB), 0.02% nickel ammonium sulfate, and 0.003% hydrogen peroxide. After stopping the staining reaction, the sections were mounted on gelatin-coated slides, air-dried, cleaned in xylene, and cover-slipped with mounting medium (Mount Quick, Daido Sangyo Co., Saitama, Japan).

For quantitative analysis, the distribution of c-Fos-immunoreactive (-ir) nuclei was plotted on a standardized chart, and the number was counted under a light microscope at a magnification of $\times 200$, as in our previous study [28]. Briefly, the spinal dorsal horn was divided into 3 specific regions to study the laminar distribution of c-Fos based on the cytoarchitectonic organization reported by Molander et al. [18]. The 3 regions were the superficial dorsal horn (laminae I–II), the proprius nucleus (laminae III–IV), and the neck of the dorsal horn (laminae V–VI). The investigator responsible for counting the c-Fos-ir nuclei was blinded to the group to which a section belonged. The number of c-Fos-ir nuclei in an animal was divided by the number of sections counted, and the result was represented as the average number of cells per section for a certain animal ($n = 5$ animals in each group).

2.5. Statistical analyses

Results are expressed as mean \pm SEM. In the electrophysiological experiment, the data are represented as median with interquartile range (IQR) except for the data of ADCCV and TPD. Comparison of the electrophysiological data between A δ - and C-fibers, and c-Fos data between the SHAM and the PINCH group, was done using the Mann–Whitney U test. The incidence of responding fibers was compared between groups with Fisher's exact probability test. Correlation was analyzed with Spearman's correlation coefficient. Data for ADCCV over time were analyzed by 2-way analysis of variance (ANOVA). Repeated 1-way ANOVA followed by Bonferroni's test was used to compare the number of CGRP- and peripherin-ir nerve fibers in the proximal, middle, and distal part of the CF. Values of $P < 0.05$ were considered significant.

3. Results

3.1. Distribution of nerve fibers in the crural fascia

Sample specimens of CGRP- and peripherin-ir axons with their nerve terminals are shown in whole-mount preparations of the CF in Fig. 3A and B. CGRP staining revealed typical bead-like swellings along the nerve fibers (Fig. 3A). There were some differences in the distribution of labeled fibers among specimens and stainings, and the distribution pattern can be summarized as follows: CGRP- and peripherin-ir fibers were densely located in the distal third of the CF in 4 of 5 preparations in both stainings (Fig. 3C and D, respectively), whereas in the remaining cases the labeled nerve fibers were observed all over the CF. There was a tendency for the labeled fibers to be distributed along the medial and lateral edge and relatively sparse in the center of the CF (Fig. 3C and D). Some fibers ran parallel to blood vessels, whereas others were not associated with them. Nerve fibers labeled with PGP 9.5-ir, on the other hand, were distributed all over the CF (3 of 4 preparations) (Fig. 3E).

In the transverse sections CGRP- and peripherin-ir fibers were more evident on the superficial side (skin side) rather than on the deeper side facing the tibialis anterior muscle. Some fibers ran transversely, parallel to the collagen fiber bundles in the CF, and others were oblique or perpendicular to them (Fig. 3F, H, and I). Few nerve fibers ran among and/or across the collagen fiber bundles in the CF (Fig. 3G).

As nerve fibers with CGRP- and peripherin-ir tended to be located densely in the distal third of the CF, we quantified the length and number of labeled fibers with CGRP- and peripherin-ir in the

proximal, middle, and distal thirds of the CF (Table 2). The length of CGRP-ir fibers and the number of CGRP- and peripherin-ir fibers were significantly longer and higher in the distal third compared with the proximal and middle thirds of the CF ($P < 0.01$ – 0.05 , repeated ANOVA followed by Bonferroni's multiple comparison test).

3.2. Electrophysiology

3.2.1. General characteristics

A total of 55 thin-fiber receptors were identified in the CF (24 A δ -fibers and 31 C-fibers). The general characteristics of the fibers are summarized in Fig. 4. The median conduction velocities of fibers were 5.02 m/s (IQR: 3.41–9.17 m/s, $n = 24$) for A δ -fibers and 0.70 m/s (IQR: 0.61–0.86 m/s, $n = 31$) for C-fibers (Fig. 4A). A clear separation between A δ - and C-fibers in the CV is recognizable, with thin-fiber receptors with CV of 1.3–2 m/s lacking.

Two-thirds of the C-fibers (16/24, 66.7%) were spontaneously active without any stimuli ($P < 0.001$, Fisher's exact probability test) (Fig. 4B). The median discharge rate was 0.05 imp/s (IQR: 0–0.37 imp/s, $n = 24$). In contrast, only 1 of 16 A δ -fibers (6.3%) was spontaneously active, and its discharge rate was 0.11 imp/s (Fig. 4C). The receptive fields of A δ -fibers were distributed over the entire CF except for the area medial to the edge of the tibial bone (Fig. 4D), whereas those of C-fibers were distributed in the distal third of the CF (Fig. 4E). The size and shape of the RFs varied. In most cases they were round or oval in shape (0.5–5 mm in diameter). The size of the RFs calculated in a pixel analysis was significantly larger for A δ -fibers (2.77 mm² (IQR: 0.83–4.13 mm²), $n = 24$) than for C-fibers (0.55 mm² (IQR: 0.20–0.81 mm²), $n = 31$, $P < 0.0001$, Mann–Whitney U test; Fig. 4F).

3.2.2. Activity-dependent change in conduction velocity

On average fascial C-fibers exhibited gradual activity-dependent slowing of CV by the first rectangular pulse of the twin stimuli (0.5 Hz, 6 repetitions; Fig. 2F). The degree of the final slowing was $-2.9\% \pm 0.6\%$. On the other hand, most A δ -fibers showed speeding ($2.1\% \pm 1.3\%$) rather than slowing, although the fluctuation was large. The degree of activity-dependent change in conduction velocity (ADCCV) over time was significantly different between A δ - and C-fibers ($P < 0.001$, 2-way ANOVA; Fig. 2F).

3.2.3. Twin pulse differences

On average, both A δ - and C-fibers exhibited slowing of CV by twin stimuli over the 6 repetitions (Fig. 2G). The size of twin pulse differences (TPD) with twin stimulus 1 (initial TPD) was $-7.9\% \pm 1.4\%$ in C-fibers and $-10.4\% \pm 2.4\%$ in A δ -fibers. The size of TPD during the 6 repetitions was significantly larger in A δ -fibers than in C-fibers ($P < 0.01$, 2-way ANOVA; Fig. 2G).

3.2.4. Mechanical response

An example of the responses of a C-afferent fiber responding to various noxious stimuli is shown in Fig. 5. Pinching of the RF in the CF with sharpened watchmaker's forceps induced a clear increase in discharges (Fig. 5B). Compression of the RF with a gradually increasing force (0–392 mN in 40 seconds) induced discharges in a roughly intensity-dependent manner up to the maximum force, followed by some discharges continuing after the end of the stimulus (Fig. 5C). This fiber was also responsive to bradykinin, cold, and heat (Fig. 5D–F), demonstrating that it was a polymodal receptor (nociceptor). A very short latency of the response to hypertonic saline suggested that the RF was located close to the surface of the CF, but not deeper in the muscles (Fig. 5G).

On average, mechano-responsive C-fibers showed a roughly intensity-dependent response pattern to the ramp mechanical stimulation (Fig. 6B). Mechano-responsive A δ -fibers also showed an intensity-dependent pattern of discharges up to 392 mN

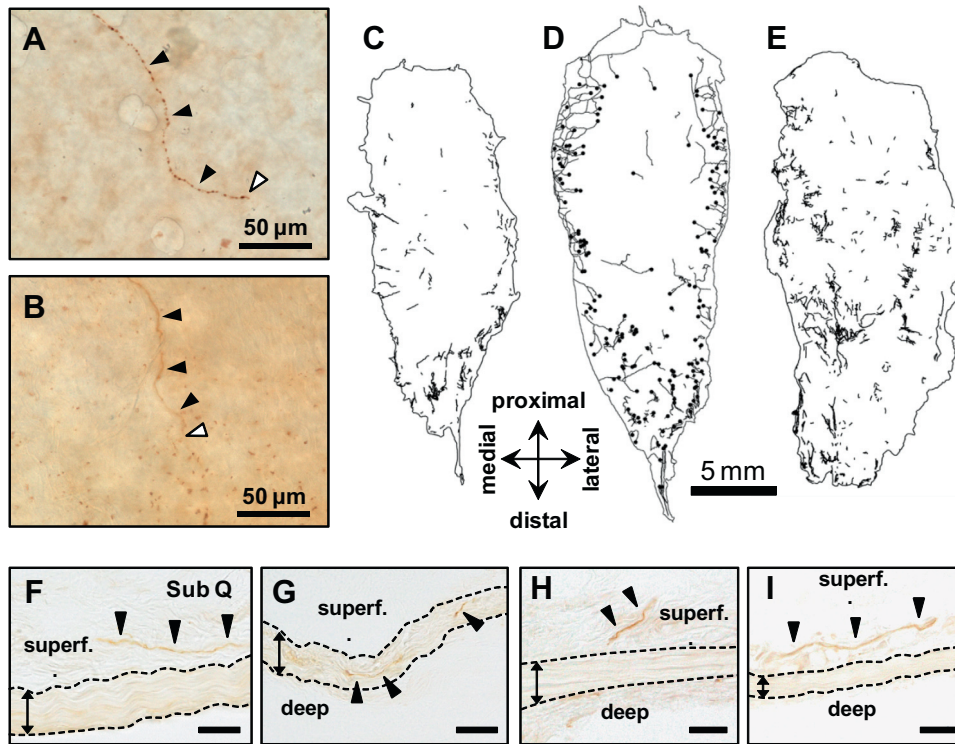


Fig. 3. CGRP- and peripherin-ir nerve fibers in the crural fascia. (A–E) Whole-mount fascia preparations. (A) A CGRP-immunoreactive (-ir) terminal axon with a long chain of varicosities and its nerve terminal. (B) A peripherin-ir receptor terminal axon and its nerve terminal. Filled arrowheads: axon of immunoreactive nerve. Open arrowheads: peripheral nerve terminal. (C–E) Distribution of nerve fibers with CGRP- (C), peripherin- (D), and PGP 9.5-ir (E) in whole-mount preparations of the CF. They were traced under a light microscope (see Methods) and drawn on a plane. In the peripherin staining, peripheral nerve terminals are indicated by dots. Note that presumptive nociceptive nerve fibers (and their terminals) labeled with CGRP- and peripherin-ir were located in the distal third of the CF, and that there was some tendency for the labeling to be dense along the medial and lateral edge and relatively sparse in the center of the CF. On the other hand, PGP 9.5-ir (general marker for nerve fibers) was distributed all over the CF. (F–I) Transverse sections. (F and G), CGRP-ir nerve fibers. Axons running parallel to the collagen bundle delineated with dashed lines (F) or in the collagen bundle (G). Note that the latter case was very rare. (H and I) Peripherin-ir nerve fibers. Axons in the superficial side (skin side) running obliquely (H) or parallel (I) to the collagen fiber bundle. Deep, deeper side (muscle side); Sub Q, subcutaneous tissue; Superf., superficial side (skin side). Scale bar = 30 μ m.

Table 1

Response characteristics of fascial thin-fiber receptors to bradykinin and thermal stimuli.

Stimulants	A δ -fibers	C-fibers	
Bradykinin 10 μ M			
Incidence	1/16 (6.3%)	13/23 (56.5%)	**
Latency (sec)	55.8 [1]	21.5 (16.2–32.0) [13]	n.a.
Magnitude (spikes)	62 [1]	96 (37–118) [13]	n.a.
Cold			
Incidence	0/15 (0%)	2/21 (9.5%)	n.s.
Threshold temp. ($^{\circ}$ C)	–	21.6, 13.1 [2]	n.a.
Magnitude (spikes)	–	18, 25 [2]	n.a.
Heat			
Incidence	0/13 (0%)	11/21 (52.4%)	**
Threshold temp. ($^{\circ}$ C)	–	36.0 (34.1–41.5) [11]	n.a.
Magnitude (spikes)	–	51 (21–74) [11]	n.a.

Fiber response incidence, latency or threshold temperature, and magnitude of response (ie, number of net evoked discharges during the stimulation period) to bradykinin (10 μ M) and thermal (cold and heat) stimuli. Numbers in brackets are the numbers of fibers analyzed. ** $P < 0.01$, Fisher's exact probability test between A δ - and C-fibers. Note the significantly higher incidence in C-fibers responding to bradykinin and heat compared with A δ -fibers. Abbreviations: n.s, not significant. n.a., not available (statistical analysis not available because of the small sample size).

(Fig. 6A), with 1 exception that showed a transient response to weaker mechanical stimulation up to 98 mN. The magnitude of the response was larger in A δ -fibers. On average, the magnitude of the mechanical response given by net evoked discharges during the stimulus period for 40 seconds was significantly higher in A δ -fibers (124.0 spikes (IQR: 25.5–393.0 spikes), $n = 16$) than in C-fibers (22.7 spikes (IQR: 7.7–54.2 spikes), $n = 24$, $P < 0.05$, Mann–Whitney U test; Fig. 6C) although the mechanical response threshold was not different between A δ -fibers (112.4 mN [IQR:

56.6–312.3 mN], $n = 16$) and C-fibers (185.4 mN (IQR: 82.3–351.3 mN), $n = 24$; Fig. 6D).

3.2.5. Response to bradykinin, cold, and heat

Response characteristics are summarized in Table 1. Bradykinin typically elicited a slowly rising and slowly decaying response in C-fibers, as shown in Fig. 5D. Thirteen of 23 C-fibers tested responded to bradykinin. In contrast, only 1 of 16 A δ -fibers, which had a relatively slow CV (2.7 m/s), was responsive to bradykinin.

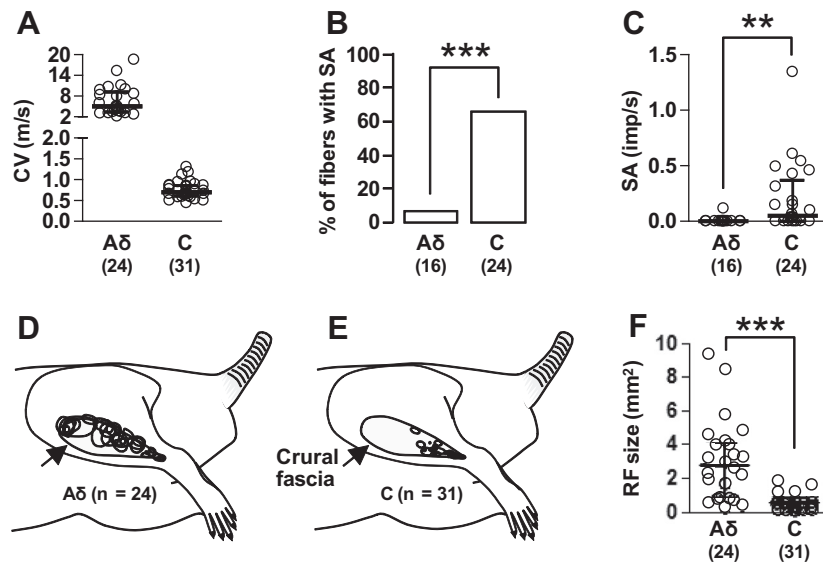


Fig. 4. General characteristics of thin-fiber receptors in the crural fascia. (A) Conduction velocity (CV; 2–20 m/s for A δ -fibers, and CV <2 m/s for C-fibers). Note a clear separation in the CV between A δ - and C-fibers; thin-fiber receptors with CV of 1.3–2 m/s were lacking. (B) Incidence of fibers with spontaneous activity (SA). (C) Discharge rate of SA. Note the significantly higher incidence (** P < 0.001, Fisher's exact probability test) and discharge rate (** P < 0.01, Mann–Whitney U test) in C-fibers than in A δ -fibers. (D and E) Receptive fields (RFs) of A δ -fibers (D) and C-fibers (E). Note that the RFs of A δ -fibers were distributed over the entire CF except the medial edge, whereas those of C-fibers were in the distal third of the CF. (F) Size of the RFs. Note the significantly larger size of RFs in A δ -fibers than in C-fibers (** P < 0.0001, Mann–Whitney U test). Data in A, C, and F are expressed as median with interquartile range (IQR).

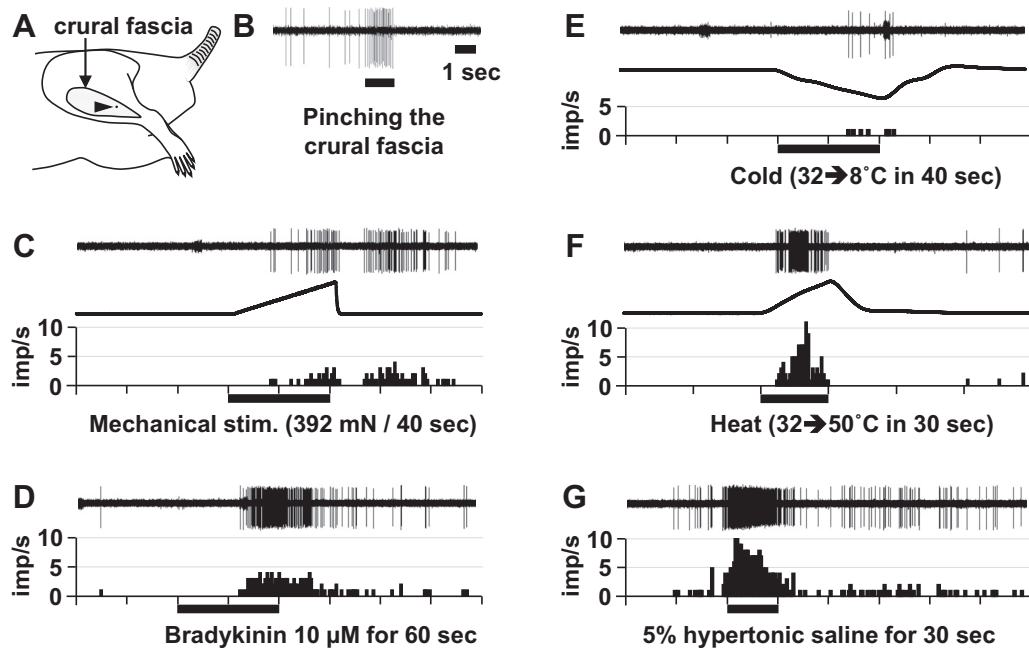


Fig. 5. Responses to various noxious stimuli of a C-afferent fiber having a receptive field in the crural fascia. (A) Receptive field of the fiber (arrowhead). Responses to pinching of the CF with sharpened watchmaker's forceps (B), quantitative ramp mechanical stimulus (392 mN in 40 seconds) (C), bradykinin 10 μ M for 60 seconds (D), cold (from 32° to 8°C in 40 seconds) (E), heat (from 32° to 50°C in 30 seconds) (F), and 5% hypertonic saline for 30 seconds (G). Bradykinin and 5% hypertonic saline were applied with a small cotton ball soaked with the solution. Filled bars under the abscissas of the histograms indicate the time point and the duration of each stimulus. CV = 0.50 m/s. This fiber was the same as one shown in Fig. 2. The short onset of the response to 5% hypertonic saline suggested that the RF of this fiber was located close to the surface of the CF, but not deeper in the muscle. Some discharges (2–5 imp/s) just before the application were due to irregular background firings after heat stimulus.

Two of 21 C-fibers were responsive to cooling to 8°C, whereas none of the A δ -fibers were. One of these C-fibers was responsive to cold, heat and mechanical stimuli, and the other only to cold and mechanical stimuli.

Of 21 C-fibers, 11 (52.4%) responded to heat with median threshold temperature of 36.0°C (IQR: 34.1–41.5°C), whereas none of the A δ -fibers did (0/13, 0%). Some fibers decreased their discharge rate before the peak temperature was reached (Fig. 5F).

On average, the heat-responsive C-fibers exhibited a temperature-dependent increase in discharge rate up to about 48°C, followed by a decrease in the rate even though the stimulus temperature was still increasing up to 50°C.

Among 21 mechano-responsive C-fibers, 14 (66.7%) were also responsive to bradykinin and/or heat, of which 9 (42.9%) responded to both bradykinin and heat (ie, polymodal receptors).

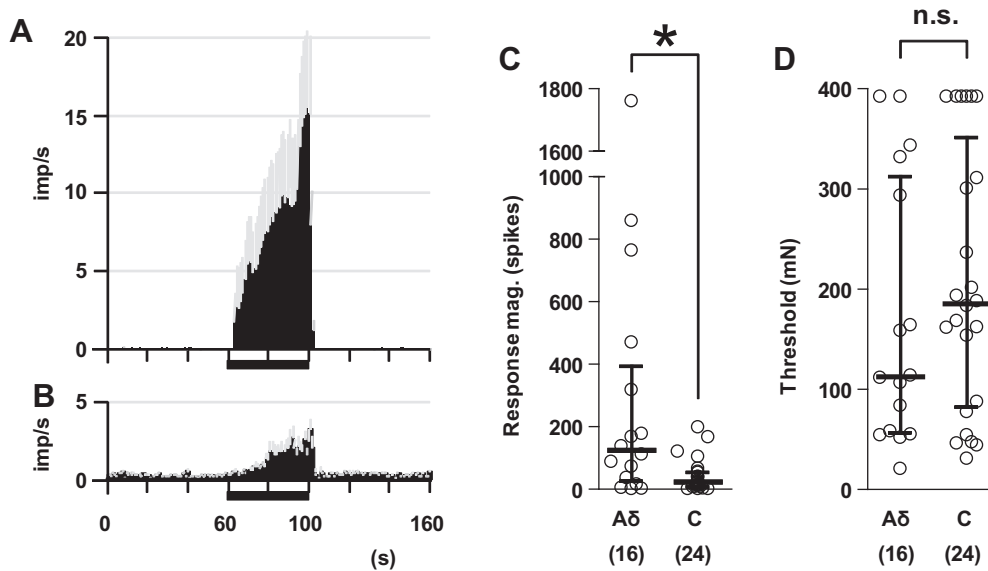


Fig. 6. Mechanical response of fascial thin-fiber receptors. (A and B) Response pattern of A δ -fibers ($n = 16$; A) and C-fibers ($n = 24$; B). The peri-stimulus time histograms were made by calculating mean discharge rate (black) + SEM (gray) of all fibers recorded (bin width: 1 second). Abscissa: time in seconds. Ordinate: discharge rate (imp/s). Filled bars under the abscissas indicate the time point and the duration of the ramp stimulus (0–392 mN in 40 seconds). Note the larger magnitude of the mechanical response in A δ -fibers than in C-fibers, although both types of thin-fibers showed roughly intensity-dependent increases in discharge rate up to the maximal stimulus intensity. (C) Magnitude of the response given by net evoked discharges during the stimulus period for 40 seconds. Note the significantly greater mechanical response in A δ -fibers than in C-fibers. (D) Threshold of the mechanical response.

Table 2

Calcitonin gene-related peptide (CGRP)-ir and peripherin-ir nerve fibers in the crural fascia.

	CGRP-ir	Peripherin-ir
Fiber length/section (μm)		
Proximal	1749.1 \pm 189.8	965.7 \pm 90.6
Middle	2041.3 \pm 150.3	1095.6 \pm 148.7
Distal	3171.4 \pm 483.5*	1843.0 \pm 499.0
No. of fibers/section		
Proximal	51.0 \pm 6.0	36.7 \pm 5.8
Middle	56.2 \pm 10.4	38.8 \pm 3.3
Distal	91.5 \pm 11.3**	65.0 \pm 7.4**

Length (upper) and number (lower) of CGRP-ir and peripherin-ir nerve fibers per section in the proximal, middle, and distal thirds of the CF are listed ($n = 6$). * $P < 0.05$, ** $P < 0.01$, 1-way repeated-measures analysis of variance followed by Bonferroni's multiple comparison test ($n = 6$). Note the significantly longer axons and higher number of immunoreactive nerve fibers in the distal part of the CF compared with other parts.

3.2.6. Differences between heat-sensitive and -insensitive C-fibers

As muscular C-fibers have been characterized by their sensitivities to heat stimulus [31], fascial C-fibers were also divided by responsiveness to heat in the present study. Heat-sensitive fascial C-fibers had slower CV than heat-insensitive ones ($P < 0.05$, Mann–Whitney U test; Fig. 7A). Other conductive indices of C-fibers (ie, ADCCV and TPD) were not different between the heat-sensitive and -insensitive fibers (Fig. 7B and C). The mechanical threshold was significantly lower ($P < 0.01$, Mann–Whitney U test; Fig. 7D) and the magnitude of the mechanical response was significantly higher ($P < 0.05$, Mann–Whitney U test; Fig. 7E) in the heat-sensitive fibers than in those that were heat-insensitive. The incidence of fibers responding to bradykinin was significantly higher in heat-sensitive fibers than in heat-insensitive ones ($P < 0.05$, Fisher's exact probability test; Fig. 7F).

3.3. c-Fos study

Repetitive pinching of the CF induced c-Fos protein expression mainly in the middle to medial superficial dorsal horn (laminae I–II) of the ipsilateral (right) side (Fig. 8A and B). No obvious immu-

noreactivity was found in laminae III–VI. Therefore, the analysis of the number of c-Fos-ir nuclei was focused on laminae I–II. The number of c-Fos-ir nuclei was significantly higher in the PINCH group than in the SHAM group at spinal segments L2–L4 ($P < 0.05$, Mann–Whitney U test; Fig. 8C). The expression was most prominent and peaked at segment L3 (6.6 \pm 1.9 nuclei in the SHAM group vs 15.4 \pm 2.0 nuclei in the PINCH group). When comparing data between the ipsilateral and contralateral sides of the corresponding spinal segments, significant differences were detected at segments L3 and L4 in the PINCH group ($P < 0.01$ at L3, and $P < 0.05$ at L4, Mann–Whitney U test) and at segment L2 in the SHAM group ($P < 0.05$, Mann–Whitney U test).

On the contralateral side, there was no significant difference in the number of c-Fos-ir nuclei between the SHAM and PINCH groups at any of the segments analyzed, from L1 to L5 (Fig. 8C).

4. Discussion

4.1. Methodological considerations

We used the crural fascia (CF) to examine the peripheral and spinal mechanisms of nociception originating from the muscle fascia. The CF is thick and binds to ankle extensor muscles via loose connective tissue. This feature allowed us to identify a mechanically sensitive RF and to stimulate it alone using sharpened forceps, without affecting any muscles underneath the fascia.

4.2. Distribution of thin fibers and presumptive nociceptive nerve fibers

Quantitative analyses of nerve fibers labeled with CGRP- and peripherin-ir revealed that these peptidergic and non-peptidergic fibers were densely distributed in the distal third. This distribution of labeled fibers fits quite well with that of recorded fascial C-fibers. Because chemical destruction of C-fibers by treatment with capsaicin eliminates most CGRP- and SP-ir nerve fibers [36], the majority of these peptidergic fibers may be C-fibers and may contribute to nociception and pain to some degree. In the present study we used a non-peptidergic neural marker of C-fibers,

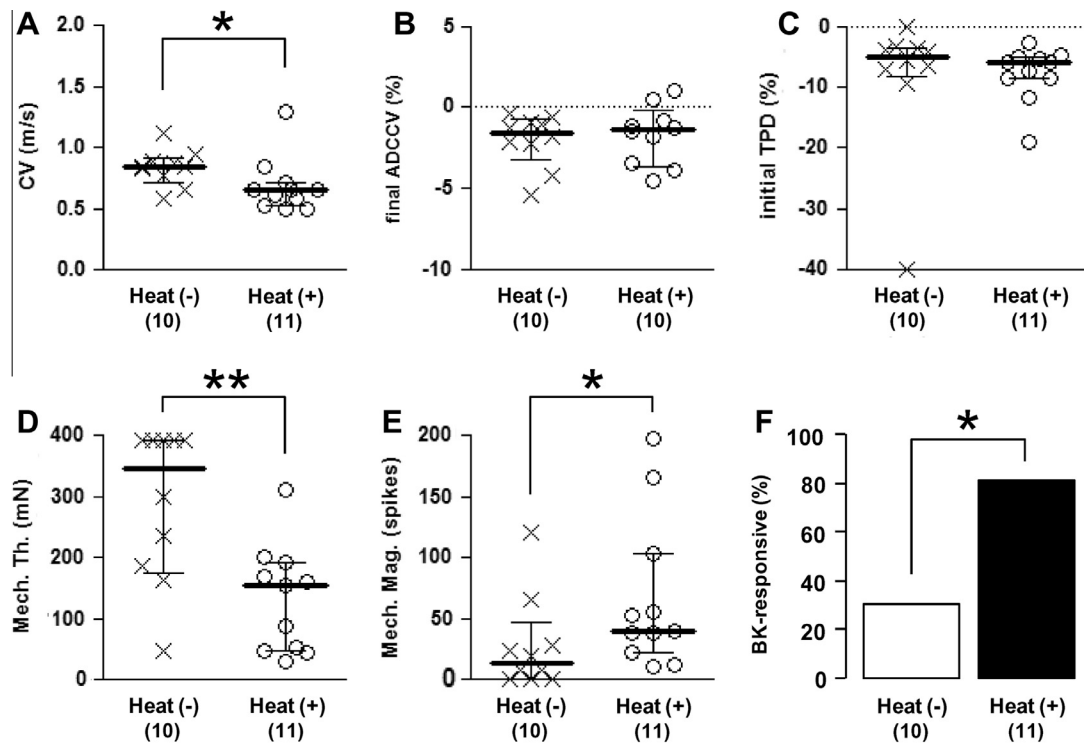


Fig. 7. Different characteristics of heat-sensitive and -insensitive fascial C-fibers. (A–C) Axonal properties between heat-sensitive and -insensitive C-fibers. Conduction velocity (A), ADCCV (B), and TPD (C). Note a significantly slower CV in heat-sensitive C-fibers ($*P < 0.05$, Mann–Whitney U test). (D and E) Mechanical response. Mechanical threshold (D) and magnitude of the response (E). Note significantly lower threshold and larger magnitude of the response in heat-sensitive C-fibers ($**P < 0.01$ and $*P < 0.05$, Mann–Whitney U test). (F) Incidence of fibers responding to bradykinin. Note significantly higher incidence of bradykinin-responsive fibers in heat-sensitive C-fibers ($*P < 0.05$, Fisher's exact probability test).

peripherin, which is a type III intermediate filament expressed in neurons extending to the peripheral nervous system [15]. The overlap of the location of labeled fibers and the distribution of the RF of C-fibers described above may suggest that these labeled nerve fibers were the substrates for the recorded nerve fibers.

In our whole-mount fascia preparations, there was a tendency for nerve fibers with CGRP- and peripherin-ir to be observed along the medial and lateral borders and to be relatively sparse in the center of the CF. This tendency was probably not due to poor permeability of antibodies for staining, as PGP 9.5-ir was observed over the entire CF. The labeling along the lateral edge of the CF may have been a substrate of A δ -fibers, because the RFs of A δ -fibers were located along the lateral edge whereas those of C-fibers were located exclusively in the distal third of the CF. The different location of RFs of A δ - and C-fibers from the same peroneal branches may be due to the different receptive properties of these 2 receptor classes (ie, A δ -fibers for mechanical nociception and C-fibers mainly for polymodal nociception). The true reason for this remains a question for future study. The medial edge, on the other hand, may be innervated by other nerve branches, as RFs of neither A δ - nor C-fibers from the peroneal nerve were observed in electrophysiological recordings.

Almost no labeling with presumed nociceptive nerve fibers was seen in the collagen fiber bundles in the CF. Similarly, substance P-ir fibers, which are assumed to be nociceptive, are also absent in the middle layer of the TLF, in which massive collagen fiber bundles exist [11,34]. The absence of nociceptive nerve fibers in such collagenous regions that may be subjected to great force transmission during movement would be reasonable, as has been shown in other collagen-rich structures such as joint cartilage [26] or intervertebral discs [7]. An alternative explanation for this would be absence of cells in collagenous tissue that produce neurotrophic factor.

4.3. Differential roles of fascial A δ - and C-fibers

In the present study, general characteristics and conductive and receptive properties of peripheral thin-fiber receptors in the CF was systematically documented for the first time. Some functional differences were seen between fascial A δ - and C-fibers.

First, background activity and the distribution of RF differed. A higher incidence of background activity was observed in fascial C-fibers than in A δ -fibers, although the discharge frequency was low on average and comparable to that in our previous experiments in the skin [29] and the muscle [30]. The size of individual RFs and the area covered by the RFs in the CF were larger for A δ -fibers than for C-fibers.

Second, axonal conductive properties differed. Fascial A δ -fibers exhibited speeding of CV by repetitive electrical stimuli, whereas C-fibers exhibited slowing. Speeding of CV has been reported in cutaneous C-fiber low-threshold mechanoreceptors, which are a type of non-nociceptors [29], but not in cutaneous A δ -fibers [35]. The different directions of the CV changes in A δ - and C-fibers might be attributable to the different tissues tested or different protocols in electrical stimulation. Because activity-dependent change in CV is assumed to be regulated by the availability of voltage-gated sodium channels (Na $_v$) [3], the expression profiles of available Na $_v$ (especially, Na $_v$ 1.7–1.9) may differ between fascial A δ - and C-fibers [2].

Mechano-responsive C-fiber afferents in the CF exhibited slowing in TPD. This was more pronounced in A δ -fibers. These changes in TPD fit well with a previous finding that all non-myelinated afferents in the skin exhibited slowing in TPD, whereas sympathetic efferents exhibited speeding [23].

Third, the responsiveness to various (noxious) stimuli was largely different. The mechanical response of the majority of fascial A δ -fibers was roughly intensity dependent up to the noxious level,

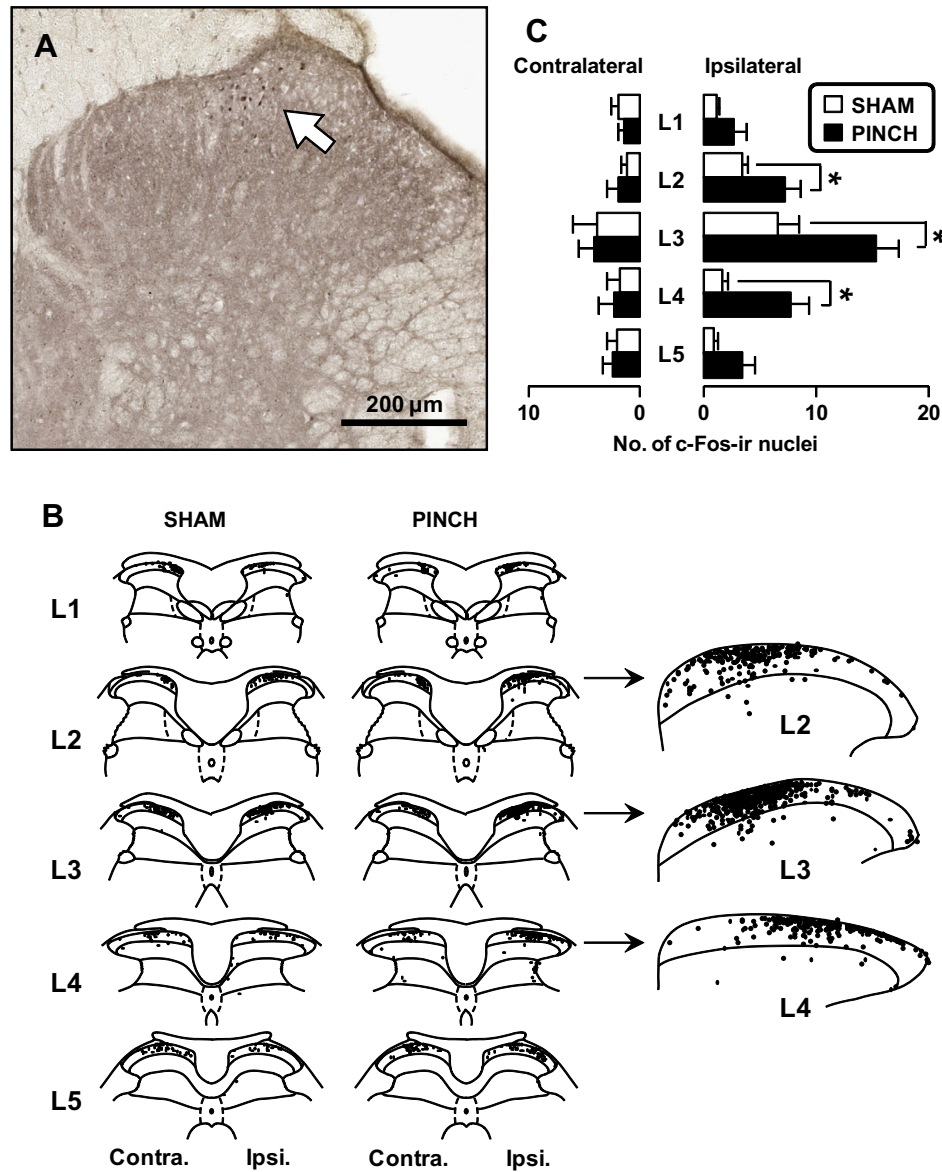


Fig. 8. c-Fos protein expression in the spinal dorsal horn in response to noxious pinching of the crural fascia. (A) Photograph of an ipsilateral spinal cord section at segment L3 taken from an animal with noxious fascial pinch. Thickness: 40 μ m. Note an intense c-Fos-immunoreactive (-ir) nuclei in the middle to medial superficial dorsal horn corresponding to laminae I–II (indicated by white arrow). (B) Distribution of c-Fos-positive neurons in the spinal dorsal horn. c-Fos-ir nuclei in each section was plotted on a standardized chart. A total of 30 sections (6 sections from each animal \times 5 rats in each group) was superimposed for each image. An intense expression of c-Fos-ir nuclei was found in the superficial laminae of the dorsal horn at segments L2 to L4. The expanded images are shown in the right side indicated by arrows. (C) Segmental distribution of c-Fos-ir nuclei in the superficial laminae I to II of animals with (PINCH, $n = 5$) and without (SHAM, $n = 5$) pinching of the CF. Note that the number was significantly higher at segments L2 to L4, and that the distribution was bell shaped, with its peak at segment L3. * $P < 0.05$, Mann–Whitney U test.

and the response magnitude was much larger, whereas noxious chemical and heat-sensitive fibers were less frequent among A δ -fibers. Together with the intensity-dependent pattern of the mechanical response and the lower chemical and heat sensitivities, this seems to show that A δ -fibers in the CF behave like mechanical nociceptors. On the other hand, noxious chemical and heat sensitivities were higher in C-fibers, although the mechanical response was small. Thus, 43% of C-fibers were polymodal receptors (nociceptors) responding to mechanical, chemical, and heat stimuli, whereas none of the A δ -fibers were the polymodal type.

4.4. C-fiber afferents in the fascia

When fascial C-fibers were divided by their responsiveness to heat stimulus, heat-sensitive ones, which are most likely to be

polymodal receptors (nociceptors), exhibited different features from heat-insensitive ones, characterized by slower CV, higher mechanical sensitivity, and higher incidence of bradykinin-sensitive fibers. Similar relationships between heat-sensitive and -insensitive fibers are also observed in muscular C-fibers [31], although the mechanical response magnitude is lower in heat-sensitive fibers in the muscle. Thus the polymodal receptor (nociceptor) is a functionally distinct component of C-fibers in the fascia as well as in the muscle.

A striking feature of fascial C-fibers is their higher mechanical response threshold. The threshold in the fascia (namely, 185.4 mN) was shown to be more than twice as high as in the skin [29] and the muscle [30], although different experimental set-ups were used in those studies (ie, ex vivo vs in vivo, with or without hard backing against the mechanical stimulation, respectively).

General characteristics such as conduction velocity and background activity in fascial C-fibers seem not to differ from those of other tissues, as reported in our previous studies [29,30].

4.5. Spinal projection of nociceptive input from the fascia

Noxious pinching over the CF yielded significant increases in c-Fos protein expression at spinal segments L2–L4, peaking at L3. The segmental distribution of neurons receiving inputs from the CF looks to be comparable to the one from skin covering the anterior surface of the lower leg [33]. In human psychophysical studies, electrical stimulation at the depth of forearm fascia induced a dull and uncomfortable sensation, whereas localized sharp pain was induced at the depth of skin [13]. Although we cannot tell the neural mechanism for the difference, a broader pattern of terminations of a single fascial afferent in the spinal cord would be a plausible explanation for the poorly localized description of fascial pain compared with skin pain. This point is a matter for future study.

The c-Fos expression in response to noxious pinching of the CF was highly localized in the middle to medial part of the superficial laminae (laminae I–II). The mediolateral and laminar distribution was similar to our previous observation in ankle extensor muscles with DOMS after lengthening contraction, although the densest c-Fos expression was observed in L4 in that case [28]. In the present experiment, we recorded single-fiber activities from the peroneal nerve, which mainly projects to L4 to L5 [17,21,24]. Thus, the CF may be innervated additionally by other nerve branches projecting to segments L2 to L3. The saphenous and femoral nerves are possible candidates, judging from the location and the patterns of spinal termination [17,24,37].

4.6. Role of fascia as a sensory tissue/organ

The physiological and anatomical roles of the “second skeleton,” fascia, as a supportive tissue/organ, have been well established [22]. Recently, Schleip et al hypothesized that the active fascial contractility observed *in vitro* may contribute to musculoskeletal biomechanics [25]. However, a possible role of fascia as a nociceptive sensory tissue/organ has not been explored, although muscle fascia has long been assumed to be important not only as an origin of nociception and pain, but also as a target tissue for treatment in patients with myofascial pain in some clinical practices (eg, acupuncture, manual therapy). Our present study together with previous reports [9,10,27,34] further support the notion that the muscle fascia is important as a nociceptive sensor, not only in physiological conditions but also in hyperalgesic, painful conditions of the myofascial structure.

4.7. Conclusion

In summary, nerve fibers labeled with CGRP- and peripherin-ir were distributed in the CF; thin-fiber receptors responding to noxious stimuli existed in the CF; and noxious pinching of the CF induced c-Fos protein expression in the superficial dorsal horn. These results further strengthen the supposition that muscle fascia is not just a supportive tissue surrounding the muscle, but is a nociceptive sensory tissue/organ.

Conflict of interest statement

The authors declare that there are no conflicts of interest related to the study.

Acknowledgments

We thank Dr. K. Katanosaka for his helpful advice in this study. This work was funded by the IASP Early Career Grant, the Nagoya University Science Foundation, Research Foundation for Oriental Medicine, Grant-in-Aid for Young Scientists (A) (23689033) and Grant-in-Aid for challenging Exploratory Research (24659106) from the Japan Society for the Promotion of Sciences. Part of this work was performed in a collaborative research project between the Nagoya University and Vitacain Pharmaceutical Co. Ltd.

References

- [1] Bove GM, Light AR. Unmyelinated nociceptors of rat paraspinal tissues. *J Neurophysiol* 1995;73:1752–62.
- [2] Cummins TR, Sheets PL, Waxman SG. The roles of sodium channels in nociception: implications for mechanisms of pain. *PAIN[®]* 2007;131:243–57.
- [3] De Col R, Messlinger K, Carr RW. Conduction velocity is regulated by sodium channel inactivation in unmyelinated axons innervating the rat cranial meninges. *J Physiol* 2008;586:1089–103.
- [4] De Col R, Messlinger K, Carr RW. Repetitive activity slows axonal conduction velocity and concomitantly increases mechanical activation threshold in single axons of the rat cranial dura. *J Physiol* 2012;590:725–36.
- [5] Deising S, Weinkauff B, Blunk J, Obreja O, Schmelz M, Rukwied R. NGF-evoked sensitization of muscle fascia nociceptors in humans. *PAIN[®]* 2012;153:1673–9.
- [6] Feng B, Gebhart GF. Characterization of silent afferents in the pelvic and splanchnic innervations of the mouse colorectum. *Am J Physiol Gastrointest Liver Physiol* 2011;300:G170–80.
- [7] Garcia-Cosamalon J, del Valle ME, Calavia MG, Garcia-Suarez O, Lopez-Muniz A, Otero J, Vega JA. Intervertebral disc, sensory nerves and neurotrophins: who is who in discogenic pain? *J Anat* 2010;217:1–15.
- [8] Gee MD, Lynn B, Cotsell B. Activity-dependent slowing of conduction velocity provides a method for identifying different functional classes of C-fibre in the rat saphenous nerve. *Neuroscience* 1996;73:667–75.
- [9] Gibson W, Arendt-Nielsen L, Taguchi T, Mizumura K, Graven-Nielsen T. Increased pain from muscle fascia following eccentric exercise: animal and human findings. *Exp Brain Res* 2009;194:299–308.
- [10] Hoheisel U, Taguchi T, Treede RD, Mense S. Nociceptive input from the rat thoracolumbar fascia to lumbar dorsal horn neurones. *Eur J Pain* 2011;15:810–5.
- [11] Hoheisel U, Taguchi T, Mense S. Nociception: the thoracolumbar fascia as a sensory organ. In: Schleip R, Findley TW, Chaitow L, Huijing PA, editors. *Fascia: the tensional network of the human body: the science and clinical applications in manual and movement therapy*. Churchill Livingstone: Elsevier; 2012. p. 95–101.
- [12] Itoh K, Kawakita K. Effect of indomethacin on the development of eccentric exercise-induced localized sensitive region in the fascia of the rabbit. *Jpn J Physiol* 2002;52:173–80.
- [13] Itoh K, Okada K, Kawakita K. A proposed experimental model of myofascial trigger points in human muscle after slow eccentric exercise. *Acupunct Med* 2004;22:2–13.
- [14] Kirillova I, Rausch VH, Tode J, Baron R, Janig W. Mechano- and thermosensitivity of injured muscle afferents. *J Neurophysiol* 2011;105:2058–73.
- [15] Lariviere RC, Nguyen MD, Ribeiro-da-Silva A, Julien JP. Reduced number of unmyelinated sensory axons in peripherin null mice. *J Neurochem* 2002;81:525–32.
- [16] Mense S. Nociception from skeletal muscle in relation to clinical muscle pain. *PAIN[®]* 1993;54:241–89.
- [17] Molander C, Grant G. Laminar distribution and somatotopic organization of primary afferent fibers from hindlimb nerves in the dorsal horn. A study by transganglionic transport of horseradish peroxidase in the rat. *Neuroscience* 1986;19:297–312.
- [18] Molander C, Xu Q, Grant G. The cytoarchitectonic organization of the spinal cord in the rat. I. The lower thoracic and lumbosacral cord. *J Comp Neurol* 1984;230:133–41.
- [19] Nakamura M, Nishiwaki Y, Ushida T, Toyama Y. Prevalence and characteristics of chronic musculoskeletal pain in Japan. *J Orthop Sci* 2011;16:424–32.
- [20] Nasu T, Taguchi T, Mizumura K. Persistent deep mechanical hyperalgesia induced by repeated cold stress in rats. *Eur J Pain* 2010;14:236–44.
- [21] Panneton WM, Gan Q, Juric R. The central termination of sensory fibers from nerves to the gastrocnemius muscle of the rat. *Neuroscience* 2005;134:175–87.
- [22] Purslow PP, Delage JP. General anatomy of the muscle fasciae. In: Schleip R, Findley TW, Chaitow L, Huijing PA, editors. *Fascia: the tensional network of the human body: the science and clinical applications in manual and movement therapy*. Churchill Livingstone: Elsevier; 2012. p. 5–10.
- [23] Ringkamp M, Johaneck LM, Borzan J, Hartke TV, Wu G, Pogatzki-Zahn EM, Campbell JN, Shim B, Schepers RJ, Meyer RA. Conduction properties distinguish unmyelinated sympathetic efferent fibers and unmyelinated primary afferent fibers in the monkey. *PLoS One* 2010;5:e9076.

- [24] Rivero-Melian C. Organization of hindlimb nerve projections to the rat spinal cord: a choleragenoid horseradish peroxidase study. *J Comp Neurol* 1996;364:651–63.
- [25] Schleip R, Naylor IL, Ursu D, Melzer W, Zorn A, Wilke HJ, Lehmann-Horn F, Klingler W. Passive muscle stiffness may be influenced by active contractility of intramuscular connective tissue. *Med Hypotheses* 2006;66:66–71.
- [26] Sofat N, Ejindu V, Kiely P. What makes osteoarthritis painful? the evidence for local and central pain processing. *Rheumatology (Oxford)* 2011;50:2157–65.
- [27] Taguchi T, Hoheisel U, Mense S. Dorsal horn neurons having input from low back structures in rats. *PAIN®* 2008;138:119–29.
- [28] Taguchi T, Matsuda T, Tamura R, Sato J, Mizumura K. Muscular mechanical hyperalgesia revealed by behavioural pain test and c-Fos expression in the spinal dorsal horn after eccentric contraction in rats. *J Physiol* 2005;564:259–68.
- [29] Taguchi T, Ota H, Matsuda T, Murase S, Mizumura K. Cutaneous C-fiber nociceptor responses and nociceptive behaviors in aged Sprague-Dawley rats. *PAIN®* 2010;151:771–82.
- [30] Taguchi T, Sato J, Mizumura K. Augmented mechanical response of muscle thin-fiber sensory receptors recorded from rat muscle-nerve preparations *in vitro* after eccentric contraction. *J Neurophysiol* 2005;94:2822–31.
- [31] Taguchi T, Sato J, Mizumura K. Different sensitivities to chemical and mechanical stimulations in heat-sensitive and -insensitive C-fiber sensory receptors recorded from rat muscle-nerve preparation *in vitro*. *Jpn J Physiol* 2005;55:S228.
- [32] Taguchi T, Yasui M, Mizumura K. Thin-fiber sensory receptors identified in the rat crural fascia. *Neurosci Res* 2011;71:e156.
- [33] Takahashi Y, Nakajima Y. Dermatomes in the rat limbs as determined by antidromic stimulation of sensory C-fibers in spinal nerves. *PAIN®* 1996;67:197–202.
- [34] Tesarz J, Hoheisel U, Wiedenhofer B, Mense S. Sensory innervation of the thoracolumbar fascia in rats and humans. *Neuroscience* 2011;194:302–8.
- [35] Thalhammer JG, Raymond SA, Popitz-Bergez FA, Strichartz GR. Modality-dependent modulation of conduction by impulse activity in functionally characterized single cutaneous afferents in the rat. *Somatosens Mot Res* 1994;11:243–57.
- [36] Tsukagoshi M, Funakoshi K, Goris RC, Kishida R. Differential distribution of nerve fibers immunoreactive for substance P and calcitonin gene-related peptide in the superficial and deep muscle layers of the dorsum of the rat. *Brain Res Bull* 2002;58:439–46.
- [37] Woolf CJ, Fitzgerald M. Somatotopic organization of cutaneous afferent terminals and dorsal horn neuronal receptive fields in the superficial and deep laminae of the rat lumbar spinal cord. *J Comp Neurol* 1986;251:517–31.
- [38] Zimmermann K, Hein A, Hager U, Kaczmarek JS, Turnquist BP, Clapham DE, Reeh PW. Phenotyping sensory nerve endings *in vitro* in the mouse. *Nat Protoc* 2009;4:174–96.
- [39] Zimmermann M. Ethical guidelines for investigations of experimental pain in conscious animals. *PAIN®* 1983;16:109–10.